

1 **Gas sampling efficiencies and aerodynamic characteristics of a**
2 **laboratory wind tunnel for odour measurement**

3
4 J. H. Sohn¹; R. J. Smith²; N. A. Hudson¹; H. L. Choi³

5
6 ¹Sustainable Intensive Systems, Department of Primary Industry & Fisheries, Queensland, Australia; e-
7 mail of the corresponding author: jaeho.sohn@dpi.qld.gov.au

8 ²Faculty of Engineering & Surveying, University of Southern Queensland, Toowoomba, Queensland,
9 Australia; e-mail: smithrod@usq.edu.au

10 ³Department of Animal Biotechnology, Seoul National University, Seoul, Korea; e-mail:
11 chlast@snu.ac.kr

12
13 **Abstract**

14 The rate of odour emission depends on meteorological factors, such as wind speed,
15 humidity and temperature, but no wind tunnels control these factors adequately. A
16 novel laboratory wind tunnel was developed that can control airflow rate. The gas
17 recovery efficiency of the tunnel was evaluated and the aerodynamic characteristics
18 were then examined to further assess its performance. Gas recovery efficiencies
19 ranged from 62 to 107 % with an average of 81 %. The optimal performance of the
20 tunnel (gas recovery efficiency of 89 %) occurred at an airflow rate and CO supply
21 rate of 1.68 m³ min⁻¹ and 10.0 litre min⁻¹, respectively. The vertical and cross-
22 sectional wind speed profiles exhibited a substantial degree of non-uniformity. The
23 airflow was turbulent, although Reynolds numbers were low indicating it to be close
24 to laminar. The non-uniform wind speed profiles and CO concentration profiles
25 illustrate the difficulty in obtaining representative samples from which to calculate

1 emission rates. Further work is required to improve aerodynamic characteristics and
2 hence performance of the tunnel.

3

4

5 **1. Introduction**

6 One of the main problems in monitoring environmental odours lies in the air
7 sampling method. There are two different methods for collecting air samples from
8 point sources or area sources of odour, namely flux chambers and wind tunnels.

9

10 The isolation flux chamber method was developed by the USEPA in 1983
11 (Klenbusch, 1986) and has been used to measure ammonia emissions from dilute pig
12 slurries (Misselbrook *et al.*, 2004), toxic gases from hazardous waste dumps (Clark *et*
13 *al.*, 1988), volatile gases from land surface (Klenbusch, 1986), and emissions of
14 nitrous oxide from farmland (Denmead, 1979).

15

16 Several factors affect the rate of emissions as sampled by a flux chamber (Smith
17 & Watts, 1994a), including: the pressure inside the chamber relative to that outside;
18 the relatively small area of emitting surface enclosed by the chamber; the suppression
19 of the turbulent transport mechanism which, under ambient conditions, transports the
20 gases away from the emitting surface; the imperfect mixing of the emissions with the
21 sweep air; and modification of the physical environment. The measured emission rate
22 depends particularly on the pressure deficit (or surplus) in the chamber. A deficit of
23 1.33 Kilopascal (kPa) resulted in a twelve-fold increase in the emission rate
24 (Denmead, 1979). Complete mixing only occurred at 2 to 9.5 cm above the air and
25 water interface. This stratification depends on the temperature of the carrier gas, the

1 surface temperature and the ambient air temperature. Variations in the thickness of the
2 stratification layer under different sampling conditions could significantly affect the
3 repeatability and reproducibility of the results (Gholson *et al.*, 1989).

4

5 Generally, the flux chamber records much lower emission rates than either wind
6 tunnel techniques, micro-met measurements, or modelling (Smith & Dalton, 1999).
7 Under field conditions, odour emission rates measured with flux chambers and wind
8 tunnel differ by up to 300 times in some cases (Jiang & Kaye, 1996).

9

10 Wind tunnels are portable, open-bottomed enclosures that are placed over the
11 emitting surface. Ambient or filtered air is drawn or blown through the tunnel in a
12 way that simulates the convective mixing and transport process present above the
13 emitting surface (Watts, 1999).

14

15 Wind tunnels have been used to estimate ammonia emissions from dairy
16 collecting yards (Misselbrook *et al.*, 1998), arable land (Loubet *et al.*, 1999b;
17 Genermont & Cellier, 1997), as well as estimating odour emissions from piggeries
18 (Smith & Dalton, 1999), feedlots (Smith & Watts, 1994b; Watts *et al.*, 1994), poultry
19 manure (Jiang & Sands, 2000), and anaerobic piggery ponds (Galvin *et al.*, 2002).

20

21 Variations in tunnel geometry include differences in the material used in
22 constructing the tunnel, the length/width ratio, the surface area sampled and the height.
23 Consequently, there are substantial effects on the exchange coefficients over the
24 emitting surface. A further complication is the variation in wind speed from one
25 device to another (Smith & Watts, 1994a).

1

2 Smith and Watts (1994b) showed that odour emission rates measured from cattle
3 feedlot were strongly correlated with wind tunnel size. The larger wind tunnel
4 consistently gave emission rates 20 % lower than the smaller tunnel. The different
5 wind velocity profiles were suggested as a possible reason for that discrepancy (Watts,
6 1999).

7

8 As it is impossible for natural ground-level wind conditions to be duplicated
9 inside a small wind tunnel, current wind tunnels are only designed to create an
10 environment where the boundary layer is well developed and convective mass transfer
11 occurs. In addition, although the odour emission rate is known to depend on
12 meteorological factors such as wind speed, humidity and temperature (Harper *et al.*,
13 1983; Smith & Watts, 1994a; Smith & Watts, 1994b), current wind tunnel systems are
14 not able to adequately control these factors.

15

16 The aerodynamic performance of a wind tunnel is considered a critical parameter
17 (Jiang & Kaye, 2001). The basic hypothesis for a wind tunnel is that the airflow is
18 completely mixed downwind of the emission chamber of the tunnel. However, the
19 wind profile results from conventional type wind tunnels show strong crosswind and
20 vertical gradients, highlighting the need for a careful analysis of the turbulence the
21 inside the tunnel (Van Belois & Anzion, 1992). Loubet *et al.* (1999a) evaluated the
22 wind tunnel that was used for estimating ammonia volatilisation from land by
23 Lockyer (1984). They showed that the vertical profiles of wind velocity and gas
24 concentration were non-uniform in the measurement section of the tunnel. The airflow
25 was far from being completely mixed leading to a recovery rate ranging from 77 to

1 87 %. Therefore, Loubet *et al.*(1999a) suggested that the design of the sampling
2 system may be of great importance in determining the average concentration
3 downwind of the emitting area for a tunnel exhibiting strong vertical gradients.

4

5 Baldo (2000) established a wind speed profile map over the emission section for
6 the wind tunnel of the University of New South Wales (Jiang *et al.*, 1995) and the
7 Lockyer hood (Lockyer, 1984). Baldo (2000) indicated that many parameters affect
8 the wind speed profile in the tunnels, including surface type, tunnel wind speed,
9 entrance characteristics, wind tunnel shape and modifications to the tunnel geometry
10 such as vanes and baffles.

11

12 A novel laboratory wind tunnel that can control airflow rate was developed to
13 measure the odour emissions under conditions similar to ambient conditions. The
14 wind tunnel was evaluated in terms of the gas recovery efficiency, and the
15 aerodynamics of the airflow inside the tunnel to further improve its performance.
16 Particular attention has been given to the effect of experimental variables such as
17 airflow rate and tracer gas, *i.e.* Carbon Monoxide, supply rates on the aerodynamics
18 and the gas recovery efficiency rates of the tunnel. It is revealed that the wind tunnel
19 increases the precision of estimates of odour emission rate but needs to be calibrated
20 to compensate for the error caused by different airflow rates and odour emission rates.

21

22

1 **2. Materials and methods**

2

3 *2.1. Description of the wind tunnel system*

4 A schematic diagram of the wind tunnel is shown in *Fig 1*. The wind tunnel
5 covers a horizontal area of 0.25 m² (0.5 m long by 0.5 m wide), and has a square
6 cross-section. Air is drawn into the tunnel by a variable speed axial-type vent fan,
7 SPEEDLOCK™ AF-300/304 S/S (Eximo® Ltd., Sydney, Australia), connected to the
8 upper part of wind tunnel. The TECO-Westinghouse® variable controller (TECO
9 Australia Pty Ltd, Sydney, Australia) was used as the fan speed controller.

10

11 A flow establishment / straightening section is placed upwind of the emission
12 section. A tapered mixing section provides mixing of the emitted gases. There is an
13 air sampling port downstream of the mixing section. The fan can produce wind speeds
14 up to 0.5 m s⁻¹ or flow rates up to 1.64 m³ min⁻¹ in the emission section. The wind
15 tunnel and all accessories were manufactured using SS 316 food-grade stainless steel.

16

17 *2.2. Sampling locations in the tunnel*

18 As the wind tunnel has the shape of a rectangular duct, the locations of points for
19 wind speed sampling were selected by the standard method of the Australian
20 Standards 4323.1 (Australian Standard 4323.1: Stationary source emission, 1995). In
21 total, there are 25 sampling points at a cross section midway along the emission
22 section of the tunnel. The vertical and lateral distances to the sampling points are
23 presented in Table 1.

24

1 For the initial measurements of gas recovery efficiency, samples were collected
2 using a one point sampling port installed at the downstream end of the mixing section
3 of the tunnel. The measured sample recovery efficiencies ranged between 20.0 % and
4 81.3 %. Subsequently, a modified sampling port with four branches and five sampling
5 holes per branch was installed in the wind tunnel. The 20 sampling points were spaced
6 quadratically across the sampling port. According to numerical simulations carried out
7 by Loubet *et al.* (1999a), this type of sampling port showed a theoretical sample
8 recovery efficiency of 100.4 %.

9

10 *2.3. Experimental design*

11 Three experiments were undertaken:

12

13 Experiment 1. The effect of sampling port design on the gas recovery efficiency
14 was identified in experiment 1. Two different types of sampling ports were tested for
15 their effect on gas recovery efficiency. Initially, a simple one-point sampling port was
16 installed centrally at the end of the mixing section and evaluated. Later, a new
17 sampling port with four branches and five quadratically spaced sampling holes per
18 branch (Loubet *et al.* 1999a), was installed in the tunnel and evaluated.

19

20 Experiment 2. The effect of airflow rate and CO supply rate on the gas recovery
21 efficiency of the tunnel was determined. Five different airflow rates, ranging from
22 0.07 to 1.69 m³ min⁻¹, were used. The gas supply rates were 2.5, 5.0, 7.5 and 10.0 litre
23 min⁻¹.

24

1 Experiment 3. Aerodynamic characteristics of the tunnel including wind speed
2 profile, turbulent intensity, and gas concentration profile, were investigated at five
3 different airflow rate, ranging from 0.07 to 1.69 m³ min⁻¹ over two different types of
4 surface. Two different types of surface, a solid surface (foam mattress) with different
5 roughness heights between 5 and 25 mm and a liquid surface (liquid piggery effluent)
6 were placed in the emissions section of the tunnel.

7

8

9 2.4. Measurements

10

11 2.4.1. Temperature and relative humidity

12 Temperature and relative humidity were measured simultaneously at the inlet and
13 outlet using the HUMITTER™ 50U/50Y(X) integrated humidity and temperature
14 transmitter (Vaisala® Ltd., Melbourne, Australia). Remote I/O module ADAMS
15 4000™, was used to collect these data (Advantech® Australia Ltd., Sydney, Australia).
16 Dedicated operating software was developed for real-time monitoring of the tunnel
17 and data logging using Labview™ Ver. 5.1 (National Instrument®, USA). Each
18 measurement was made over a 900 s period at a sample rate of 20 Hz.

19

20 2.4.2. Carbon monoxide concentration

21 Pure carbon monoxide (CO) gas was used as a tracer gas for the gas recovery
22 efficiency experiment. The CO gas was introduced into the tunnel through perforated
23 tubes. CO concentration was 200 ppm (BOC® Australia, Brisbane, Australia). Four
24 tubes were laid out under the emission section of the tunnel in parallel rows. Each
25 tube had 50 tiny holes per metre to provide homogeneous gas emissions to the tunnel.

1 A visual flowmeter (Cole-Parmer[®], USA) and a needle valve (Swagelok[®] Ltd.,
2 Australia) were used to control the CO supply rate.

3

4 The CO concentration was measured with the 300E gas filter correlation CO
5 analyser[™] (Teledyne Instruments[®], USA) at a frequency of 10 Hz. Air was
6 continuously sampled at the sampling port and drawn to the analyser through
7 polytetrafluoroethylene (PTFE) tubes with 4 mm inner diameter (Swagelok[®] Ltd.,
8 Australia). The analyser was calibrated regularly with two reference standard CO
9 gases (BOC[®] Australia, Brisbane, Australia) at 206 and 1000 ppm. The detection limit
10 of the CO analyser was 0.04 ppm. Linearity was better than 1 % full scale for CO
11 concentrations greater than 10 ppm, and better than 0.2 ppm for lower concentrations.
12 The precision was 0.5 % of the value read.

13

14 *2.4.3. Normalisation of CO concentration*

15 To get normalised gas concentration, the mean volumetric concentration increase
16 in a section of the tunnel \bar{C}_{inc} is calculated as the ratio of the CO volumetric flow
17 injected into the tubes Q_{CO} , to the volumetric airflow in the tunnel Q (modified from
18 Loubet *et al.*, 1999a):

19

$$20 \quad \bar{C}_{inc} = \frac{Q_{CO}}{Q} \quad (1)$$

21

22 The normalized concentration is then defined as the ratio of the concentration at a
23 given position C_Z minus the background concentration C_B to the mean concentration
24 increase \bar{C}_{inc} in the same cross-section:

1

$$2 \quad C_{norm} = \frac{(C_Z - C_B)}{\bar{C}_{inc}} \quad (2)$$

3

4 2.4.4. Gas recovery efficiency rate

5 The recovery rate of the tunnel (α) was calculated using the equation (3) (modified
6 from Loubet *et al.*, 1999a).

7

$$8 \quad \alpha = \left(\frac{\bar{Q} \bar{C}_m}{A_{exp} \Phi_{exp}} \right) \quad (3)$$

9 where \bar{Q} is the mean volumetric airflow rate through the tunnel in $\text{m}^3 \text{s}^{-1}$; A_{exp} is the
10 experimental area covered by the tunnel in m^2 ; \bar{C}_m is the measured average
11 concentration in the measurement section in kg m^{-3} ; Φ_{exp} is the CO emission rate in
12 the emission section in $\text{kg m}^{-2} \text{s}^{-1}$.

13

14

15 2.4.5. Wind speed

16 The wind speed was measured with a VelocicalcTM velocity meter (TSI[®]
17 Incorporated, USA). Absolute accuracy of the wind speed meter was 1 % of full-
18 scale, which corresponded to 0.01 m s^{-1} . The probe was located as described in section
19 2.2 for the vertical wind speed profiles and cross-sectional wind speed profiles. For
20 the gas recovery efficiency trials, the probe was placed in the middle of the emission
21 section of the tunnel as a reference. As the wind speed meter gives result in standard
22 temperature and pressure condition, the wind speed was corrected by a factor $T /$
23 294.55 , where T is the ambient temperature in K.

1

2 2.4.6. *Standardisation of airflow rate*

3 The volumetric airflow rate at standard conditions (0 °C and 101.3 kPa) was then
4 calculated in accordance with ISO 10780 using equation (4) (modified from
5 AS4323.1, 1995)

6

$$7 \quad \bar{Q}_{R,0} = \bar{Q}_s \frac{(273 + 0)}{(273 + T_t)} \frac{P_s}{101.3} \quad (4)$$

8 where $\bar{Q}_{R,0}$ is the volumetric airflow rate at standard conditions (0 °C and 101.3 kPa),
9 $\text{m}^3 \text{s}^{-1}$; P_s is the absolute pressure in the tunnel, kPa; \bar{Q}_s is the mean volumetric airflow
10 rate through the tunnel, $\text{m}^3 \text{s}^{-1}$; and T_t is the tunnel temperature, °C.

11

12 2.4.7. *Turbulence Intensity*

13 The turbulence intensity, I is defined by three variables: the turbulent component
14 of the wind speed v' , the mean wind speed in the profile \bar{V} , and the maximum wind
15 speed in the profile V_{\max} , where:

16

$$17 \quad v' = \bar{V} - V \quad (5)$$

$$18 \quad I = \frac{\sqrt{v'^2}}{V_{\max}} \quad (6)$$

19

1

2 **3. Results and discussion**

3

4 *3.1. Gas recovery efficiency of the wind tunnel*

5

6 *3.1.1 Effect of sampling port design on the gas recovery efficiency*

7 The results of experiment 1 regarding the sampling port design are summarised in
8 Table 2. When the CO gas was supplied at a rate of 5.0 litre min⁻¹, the sample
9 recovery efficiency using the one point sampling port ranged from 20 % to 81 %. The
10 mean ± standard deviation (std) recovery efficiency was 49 ± 29 %. In contrast, the
11 sampling point with four branches and five quadratically spaced sampling holes per
12 branch produced a mean ± std recovery efficiency of 71 ± 11 %. The range of
13 recovery efficiencies was 64 to 90 %. This improvement is solely due to the improved
14 sampling port. Similarly, Loubet *et al.* (1999a) reported ‘simulated’ recovery
15 efficiencies of a one point and a 20 point sampling port (with a linear distribution) of
16 61 % and 89 % respectively, and of 100.4 % with a quadratic distribution. For the
17 linear distribution of sampling points, the number of sampling points per unit area will
18 decrease with distance to the centre of the duct, whereas in the case of a quadratic
19 distribution, it remains constant.

20

21

22 *3.1.2 Effect of airflow rate and gas supply rate on gas recovery efficiency*

23 The results of experiment 2 are presented in *Fig 2*. The results reveal gas recovery
24 efficiencies for individual tests ranging from 62 to 107 %, while the average result for
25 the entire data set was 81 %.

1

2 Optimal performance, that is, consistently high gas recovery efficiencies, was $89 \pm$
3 4% at an airflow rate of $1.68 \text{ m}^3 \text{ min}^{-1}$. The recovery efficiency at this optimal
4 condition is similar to or better than efficiencies reported in other studies using
5 different wind tunnel systems. Other researchers reported recovery efficiencies in a
6 range from 70% to 103% under varying tunnel geometry and operating conditions
7 (Wang *et al.*, 2001; Loubet *et al.*, 1999b; Reitz *et al.*, 1997; van der Weerden *et al.*,
8 1996; Mannheim *et al.*, 1994).

9

10 At the airflow rate of $0.89 \text{ m}^3 \text{ min}^{-1}$, the tunnel showed the highest averaged gas
11 recovery efficiency rate of $95 \pm 16 \%$. However, this result was leveraged by
12 overestimated recovery efficiencies of 107% and 104% . It also included high
13 variability as shown by the standard deviation value.

14

15 Gas recovery efficiencies at CO gas supply rates of 2.5, 5.0, 7.5 and 10.0 litre min⁻¹
16 were $80 \pm 17 \%$, $71 \pm 11 \%$, $81 \pm 14 \%$ and $92 \pm 10 \%$ respectively.

17

18 The gas recovery efficiencies and hence estimates of emission rates, made from
19 the concentrations measured in the tunnel, are closely related to the uniformity of
20 concentration profiles and the degree of mixing developed inside the tunnel. The
21 results of this study suggest that the wind tunnel will give estimates of the odour
22 emission rate with a significantly improved level of accuracy. However, the wind
23 tunnel needs to be calibrated to compensate for the different recovery efficiencies
24 caused by different airflow rates. To get more reliable and repeatable results,

1 improvements to the wind tunnel to improve mixing downstream of the emissions
2 section will be required.

3
4

5 *3.2. Aerodynamic characteristics of the wind tunnel*

6

7 *3.2.1. Wind speed profiles*

8 The mean vertical profiles of wind speed measured at the centre of the emission
9 section of the tunnel, over the solid surface and over the liquid surface are presented
10 in *Fig 3* and *Fig 4*.

11

12 While the airflow rate was increasing, the horizontal wind speed was increasing
13 accordingly. However, the wind speed profiles were not uniform regardless of the
14 airflow rate. For all of the higher airflow rates, there was a pronounced peak in the
15 profile at about 0.1 m above the bottom of the emission section for the solid surface
16 and 0.15 m for the liquid surface. The lowest wind speed was usually recorded at the
17 bottom of the profile, which had a logarithmic shape. Moreover, for any given airflow,
18 the maximum wind speed was higher over the liquid surface than over the solid
19 surface.

20

21 Compared with the wind speed profile results reported by Leyris *et al.* (2000) and
22 Loubet *et al.* (1999a), both sets of profiles indicated incomplete development of the
23 flow, caused by an insufficient straight length of ducting prior to the emission section.

24

1 The contour plot for the cross-sectional wind speed profile over the solid surface
2 is shown in *Fig 5*, and over the liquid surface in *Fig 6*. These profiles show a variation
3 in wind speed across the width of the tunnel. In each case, two zones of high wind
4 speed are observed near the centre of each half of the cross section.

5

6 One possible explanation for these flow patterns is low wind speed. Compared to
7 conventional wind tunnels operated at $0.1 - 0.5 \text{ m s}^{-1}$, the highest wind speed
8 measured at the emission section of the tunnel was 0.26 m s^{-1} . The height of the
9 emission section is 300mm. Frechen (2003) indicated that, as the wind speed is
10 influenced by the tunnel height, it was possible to increase the sweep wind speed by
11 reducing the tunnel's height. Besides, low height tunnels are advantageous due to
12 their better behaviour concerning flow pattern and vertical homogeneity. He
13 suggested that heights greater than 0.15 m should be avoided.

14

15 3.2.2. *Flow characteristics*

16 Reynolds numbers above 1×10^4 are associated with turbulent flow. The Reynolds
17 number is defined as:

18

$$19 \quad R_e = \frac{LV\rho}{\nu} \quad (7)$$

20 where R_e is the Reynolds number; L is the characteristic length of the duct in m; V is
21 the wind speed in the duct of the wind tunnel in m s^{-1} ; ρ is the density of the air in kg
22 m^{-3} ; ν is the dynamic viscosity of the air, $\text{kg m}^{-1} \text{ s}^{-1}$.

23

24 The dynamic viscosity of air at $20 \text{ }^\circ\text{C}$ is about $1.8 \times 10^{-5} \text{ kg m}^{-1} \text{ s}^{-1}$. Hence, the
25 Reynolds number was estimated to 1.4×10^4 in this wind tunnel. Therefore, the

1 airflow inside the duct is revealed to be turbulent flow. However, this number is lower
2 than the Reynolds number of between 3×10^4 and 9×10^4 presented by Loubet *et al.*
3 (1999a) for their wind tunnel. This lower Reynolds number is due mainly to the low
4 range of wind speeds that were applied in this research.

5

6 The turbulence intensity profiles over the solid surface and the liquid surface are
7 shown as a function of height in *Fig 7* and *8*, respectively. As with the wind speed
8 profiles, the vertical profiles of turbulence intensity are not uniform regardless of the
9 airflow rate and surface type. In fact, the turbulence intensity shows an inverse
10 relationship with wind speed. The highest intensity is located where wind speed is
11 lowest, that is, close to the wall of the wind tunnel. The turbulence intensity profiles
12 are similar in shape to those reported by Loubet *et al.* (1999a). However, it is
13 observed that the peak turbulence intensity over the solid surface is higher than for the
14 liquid surface for the same fan speed.

15

16 *3.2.3. Gas concentration profiles in the emission section of the tunnel*

17 The vertical CO concentration profiles measured in experiment 3 are presented in
18 *Fig 9*. The CO supply rate was 5 litre min^{-1} . The trial was done over the solid surface,
19 and the CO concentration profiles measured within the emission section of the tunnel.

20

21 The normalised CO concentration profiles showed the strong asymmetry, typically
22 seen in the results of dispersion modelling of area source emissions (for example,
23 Harris *et al.* (1996). Concentration is a maximum close to the emitting surface,
24 tapering rapidly with height above the surface. The normalised concentration profiles
25 were similar in shape for the five different airflow rates. These results are also similar

1 to the gas concentration profiles within conventional wind tunnels, reported by Loubet
2 *et al.* (1999a) and Leyris *et al.* (2000). They indicated that the asymmetry would
3 likely be independent of the wind speed in the tunnel, for a given geometric
4 configuration of the experimental area.

5
6 The presence of concentration gradients in the air stream illustrates the difficulty
7 in obtaining a representative sample from which to estimate the odour emission rate.
8 Leyris *et al.* (2000) suggested that the traditional way to calculate emission rates from
9 wind tunnel samples (equation 3) is not valid because of these concentration
10 gradients.

11 12 *3.3 Suggestions to improve the performance of the tunnel*

13 Loubet *et al.* (1999a) proposed three hypotheses are necessary for equation 3 to be
14 valid, viz: the turbulent component of the horizontal wind velocity is assumed to be
15 negligible in the inlet and the measurement section of the tunnel; the wind speed
16 profile is assumed to be constant in the cross-section of the duct; and the
17 concentration gradients in the duct are assumed to be low, so that the average
18 concentration can be estimated accurately from a sampling system with a limited
19 number of sampling points.

20
21 However the same result may be achieved more simply by designing the tunnel to
22 ensure adequate mixing of the air stream prior to sampling. The relatively high gas
23 recovery efficiencies presented earlier suggest that a substantial degree of mixing has
24 already been attained.

1 An issue of perhaps greater importance is the nature of the vertical wind speed
2 profiles in the tunnel and how the emission rates relate to ambient emissions. Jiang
3 and Kaye (2001) designed their tunnel to give a uniform wind speed profile. However,
4 the method commonly used to convert the tunnel emission rate to an equivalent
5 ambient value (Galvin *et al.*, 2004) assumes that the typical ambient logarithmic
6 profiles apply. Open tunnels such as that of Lockyer (1984) would have profiles
7 approximating ambient conditions. The tunnel examined in this study has neither a
8 uniform nor logarithmic profile. Substantial further work is required to: (i) determine
9 the most appropriate profile to apply in the tunnel, and (ii) modify the tunnel to
10 achieve the desired profile.

11

12

13 **4. Conclusions**

14 This wind tunnel is expected to be a more precise tool for odour sampling because
15 it has the potential to duplicate natural ground-level wind conditions more effectively
16 than other wind tunnels and with a capability to control airflow rates. Therefore, it
17 will be suitable for more demanding tasks like the measurement of the kinetics of
18 odour emission rates from specific odour sources. Gas recovery efficiencies in the
19 tunnel were consistently high at the higher wind speeds indicating that under these
20 conditions it will give accurate estimates of odour emission rates. Further
21 improvements in the gas recovery efficiency and in the aerodynamic performance of
22 the tunnel are possible.

23

24

1 **Acknowledgements**

2 The authors acknowledge the support of the Project Teams Research Program of
3 the University of Southern Queensland for funding the salary and operational costs of
4 the first author, and of the Queensland Department of Primary Industries & Fisheries
5 for provision of the measurement instruments.

6

7 **References**

8 **Australian Standards** (1995). Stationary source emissions (AS/NZS 4323.1).
9 Standards Australia, Sydney, Australia

10 **Baldo L J** (2000). Wind velocity profiles in odour sampling wind tunnels. Bachelor
11 of Engineering Dissertation, Faculty of Engineering & Surveying, University of
12 Southern Queensland, Toowoomba, Australia

13 **Clark J A; Schmidt C E; D'Avanzo T** (1988). Overview of applicable emission
14 measurement technologies for the measurement of volatile hazardous waste
15 emissions. International Symposium on Measurement of Toxic and Related Air
16 Pollutants, EPA/APCA, Research Triangle Park, North Carolina, 383-398

17 **Denmead O T** (1979) Chamber systems for measuring nitrous oxide emission from
18 soils in the field. Soil Science Society of America Journal, **43**, 89-95

19 **Frechen F B** (2003). State of the art of odour measurement. International Symposium
20 on Odor Measurement, Ministry of Environment, Government of Japan, 30
21 October 2003, Tokyo

22 **Galvin G; Lowe S; Atzeni M; Casey K** (2002). Spatial variability of odour
23 emissions from anaerobic piggery ponds. In Enviro 2002 Convention and
24 Exhibition & IWA World Water Congress, Melbourne

1 **Galvin G; Lowe S; Smith R** (2004). The validation of a simple Gaussian dispersion
2 model for determining odour emission rates from area sources. Developments in
3 Chemical Engineering and Mineral Processing, special issue on environment
4 and energy, **12(5/6)**, 545-558

5 **Genermont S; Cellier P** (1997). A mechanistic model for estimating ammonia
6 volatilization from slurry applied to bare soil. Agricultural and Forest
7 Meteorology, **88**, 145-167

8 **Gholson A R; Albritton J R; Jayanty R K M** (1989). Evaluation of the flux
9 chamber method for measuring volatile organic emissions from surface
10 impoundments. EPA/600/3-89/008, US Environmental Protection Agency,
11 Research Triangle Park, NC, PB89-148589

12 **Harper L A; Catchpole V R; Davis R; Weir K L** (1983). Ammonia volatilization:
13 soil, plant, and microclimate effects on diurnal and seasonal fluctuations.
14 Agronomy Journal, **75**, 212-218

15 **Harris T; Smith J N; Smith R J; Hancock N H** (1996). Vertical dispersion of
16 emissions from ground level sources: A comparison of the Lagrangian and
17 Gaussian models. Conference on Engineering in Agriculture and Food
18 Processing, Univ of Qld Gatton, Paper No SEAg 96/052

19 **Jiang J K; Bliss P J; Schultz T J** (1995). The development of a sampling technique for
20 determination of odour emission rate from areal surfaces: I. Aerodynamic
21 performance. Journal of Air and Waste Management Association, **45**, 917-922

22 **Jiang J K; Kaye R** (1996). Comparison study on portable wind tunnel system and
23 isolation chamber for determination of VOC's from areal sources. Water
24 Science and Technology, **34** (3-4), 583-589

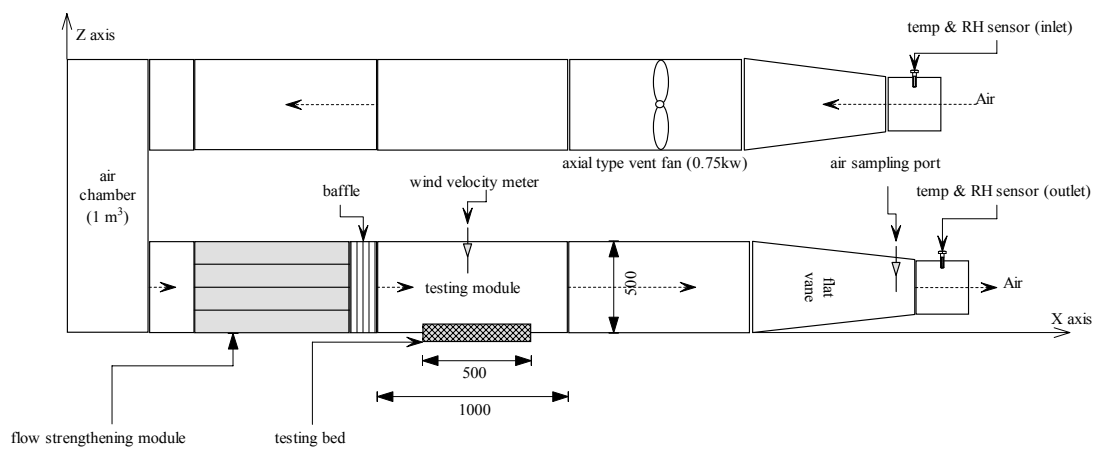
- 1 **Jiang J K; Kaye R** (2001). Chapter 5 Sampling techniques for odour measurement.
2 In odours in wastewater treatment. Modelling and Control, Eds Stuetz R;
3 Frechen F-B, IWA publishing, Padstow, Cornwall, UK, ISBN: 1 900222 46 9
- 4 **Jiang J K; Sands J R** (2000) Odour and ammonia emission from broiler farms. A
5 report for the Rural Industries Research and Development Corporation, RIRDC
6 Publication No 00/2, Kingston, ACT, Australia
- 7 **Klenbusch M R** (1986) Measurement of gaseous emission rates from land surfaces
8 using an emission isolation flux chamber, User's guide. EPA/600/8-86/008; US
9 Environmental Protection Agency, Las Vegas, USA
- 10 **Leyris C; Maupetit F; Guillot J M; Pourtier L; Fanlo J L** (2000) Laboratory study
11 of odour emissions from areal sources: evaluation of a sampling system.
12 *Analisis*, **28** (3), 199-206
- 13 **Lockyer D R** (1984). A system for the measurement in the field of losses of ammonia
14 through volatilisation. *Journal of the science of food and agriculture*, **35**, 837-
15 848
- 16 **Loubet B; Cellier P; Flura D; Genermont S** (1999a). An evaluation of the wind
17 tunnel technique for estimating ammonia volatilization from land: Part 1.
18 Analysis and improvement of accuracy. *Journal of Agricultural Engineering*
19 *Research*, **72**, 71-82
- 20 **Loubet B; Cellier P; Genermont S; Flura D** (1999b). An evaluation of the wind-
21 tunnel technique for estimating ammonia volatilization from land: Part 2.
22 Influence of the tunnel on transfer processes. *Journal of Agricultural*
23 *Engineering Research*, **72**, 83-92

- 1 **Mannheim T; Braschkat J; Marschner H** (1994). Measurement of ammonia
2 emission after liquid manure application: II. Comparison of the wind tunnel and
3 the IHF method under field conditions. *Planzernernähr, Bodenk*, **158**, 215-219
- 4 **Misselbrook T H; Pain B F; Headon D M** (1998). Estimates of ammonia emission
5 from dairy cow collecting yards. *Journal of Agricultural Engineering Research*,
6 **71**, 127-135
- 7 **Misselbrook T H; Smith K A; Jackson D R; Gilhespy S L** (2004) Ammonia
8 emissions from irrigation of dilute pig slurries. *Biosystems Engineering*, **89** (4),
9 473-484
- 10 **Reitz P; Kutzbach H D** (1997). Accuracy of wind tunnel for measuring ammonia
11 emissions after slurry application. Proceeding of the International Symposium
12 on 'Ammonia and odour emissions from animal production facilities',
13 Vinkeloord, Netherlands, 6-10 October. Published by NVTL, Rosmalen, 1997:
14 Section 2, 595-602
- 15 **Smith R J; Dalton P A** (1999). Environmental odours from Australian piggeries,
16 Australasian Environmental Engineering Conference, Auckland, New Zealand,
17 10-14 July.
- 18 **Smith R J; Watts P J** (1994a). Determination of odour emission rates from cattles
19 feedlots: Part 1, A Review. *Journal of Agricultural Engineering Research*, **57**,
20 145-155
- 21 **Smith R J; Watts P J** (1994b). Determination of odour emission rates from cattle
22 feedlots: Part 2, Evaluation of two wind tunnels of different size. *Journal of*
23 *Agricultural Engineering Research*, **58**, 231-240

- 1 **Van Belois H J; Anzion C J M** (1992). Measurement of emissions over surface areas
2 using the hood method. In *Biotechniques for air pollution abatement and odour*
3 *control policies*. Elsevier, Amsterdam, ISBN 044489263X
- 4 **Van der Weerden T; Moal J F; Martinez J; Pain B F; Guiziou F** (1996).
5 Evaluation of the wind tunnel method for measurement of ammonia
6 volatilisation from land. *Journal of Agricultural Engineering Research*, **58**, 231-
7 240
- 8 **Wang X; Jiang K; Kay R** (2001). Improvement of wind tunnel sampling system for
9 odour and VOC's. *Proceedings of 1st IWA International Conference on Odour*
10 *and VOC's*, Sydney, 2001, 147-154
- 11 **Watts P J** (1999). Development of a pig effluent emissions database and analysis of
12 promising control strategies: Final Report (Part A) Database on odour research
13 and emission rates. Pig Research and Development Corporation, Canberra,
14 ACT, Australia Project No. FSE 1/1503

1

2



3

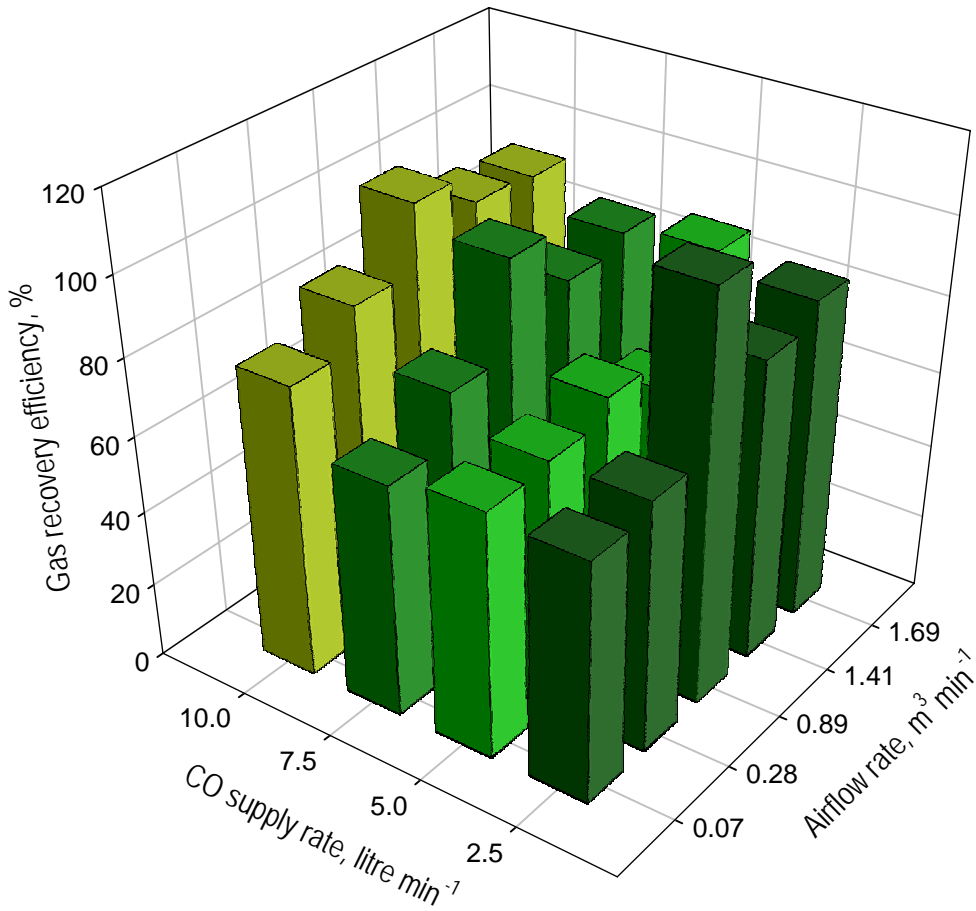
4

5

6

7

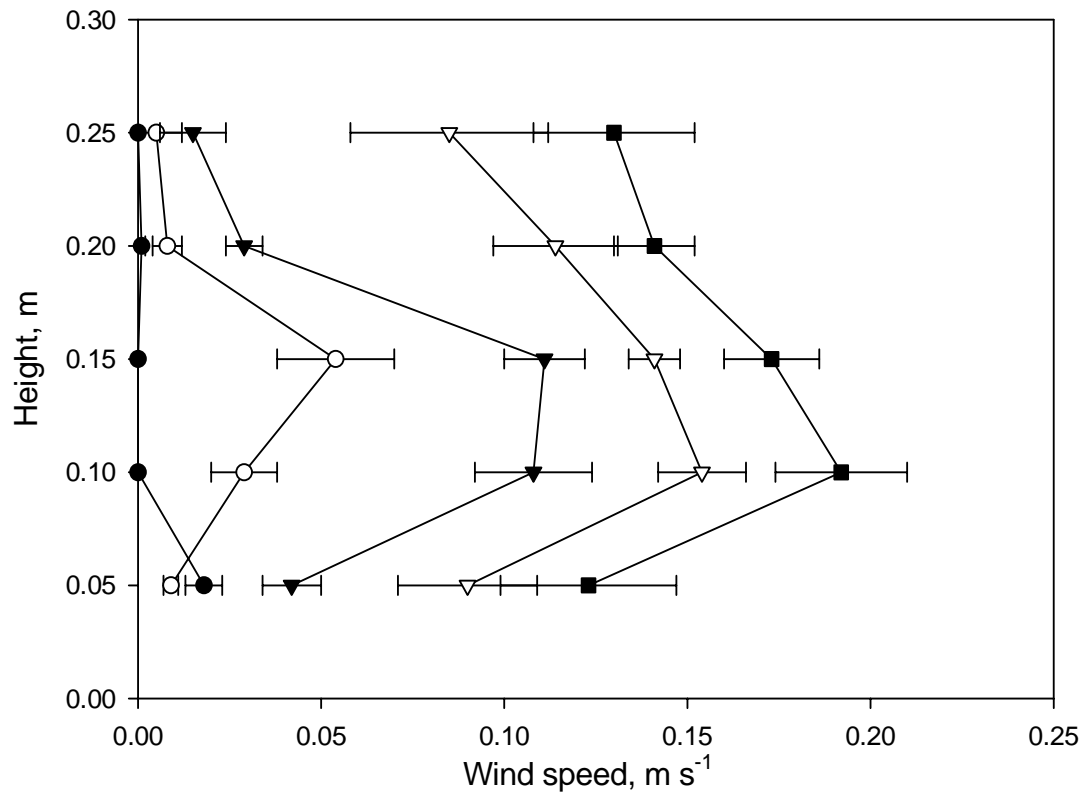
Fig 1. Schematic diagram of the wind tunnel system. It was designed to have a capability to control airflow rates from 0.07 to $1.69\text{m}^3 \text{min}^{-1}$



1
2
3
4

Fig 2. Sample recovery efficiency rates for different airflow rates and gas supply rates

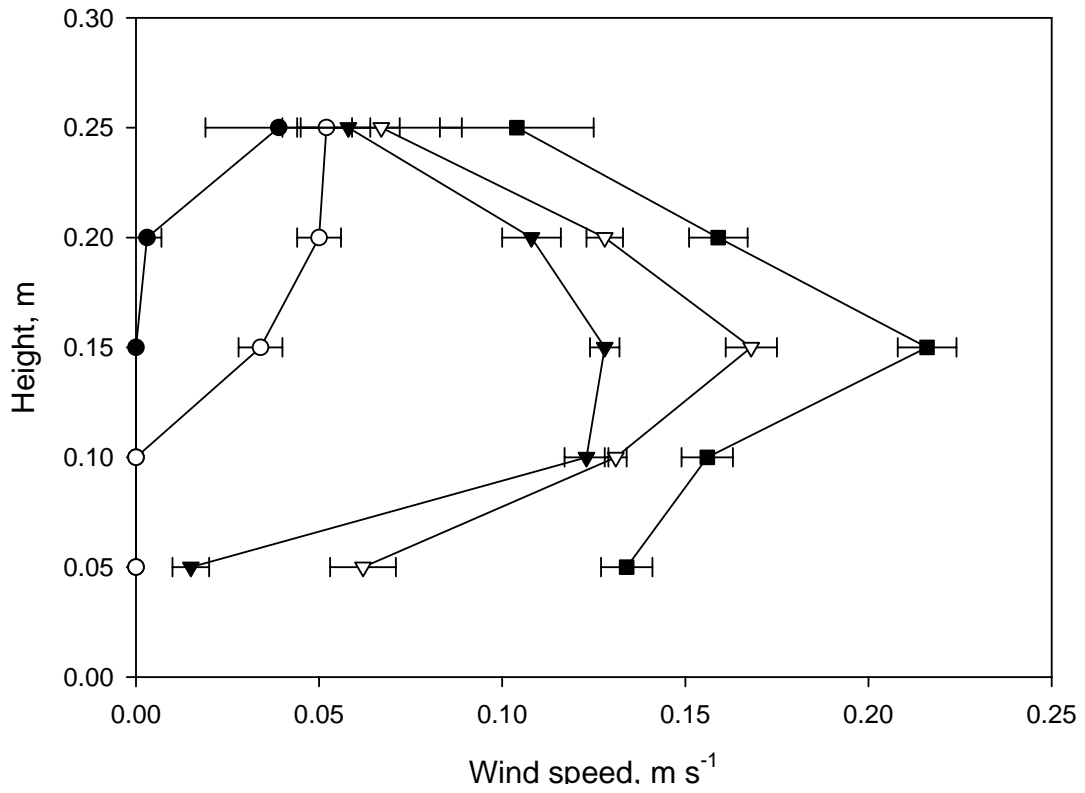
1



2

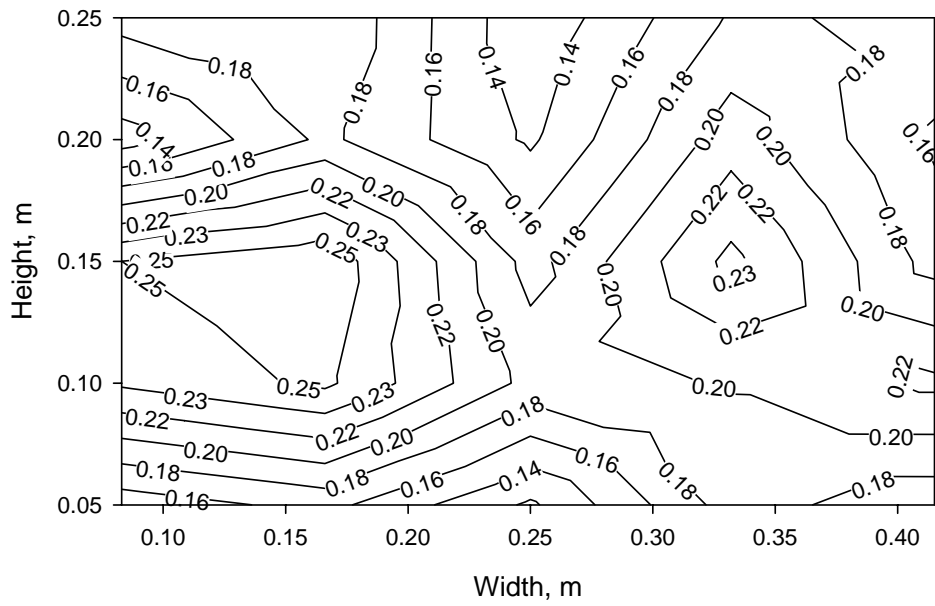
3

4 *Fig 3. Mean vertical profiles of wind speed over the solid surface for several airflow*
5 *rates: ●, 0.07 m³ min⁻¹; ○, 0.28 m³ min⁻¹; ▼, 0.89 m³ min⁻¹; ▽, 1.41 m³ min⁻¹; ■, 1.69*
6 *m³ min⁻¹ (the error bar represents the value of standard deviation)*



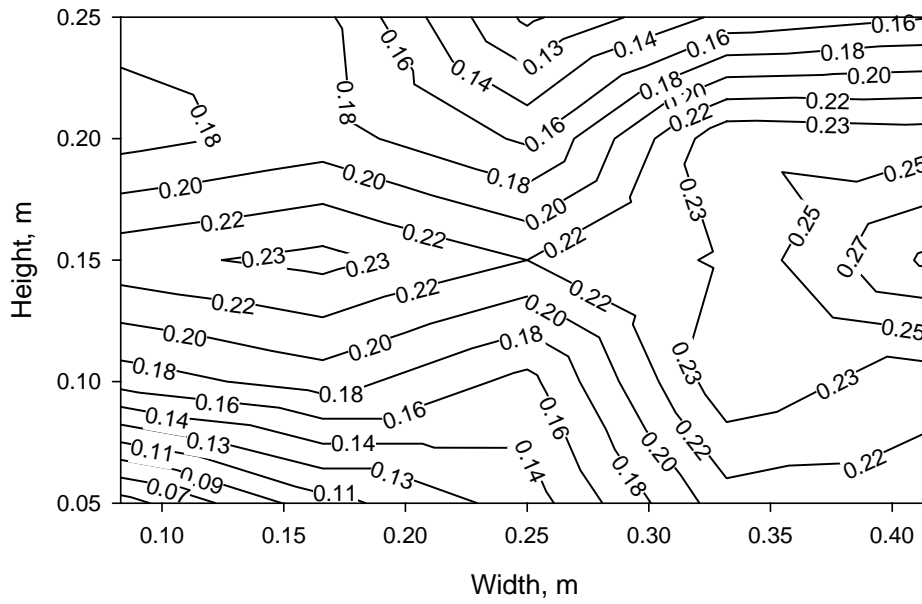
1
2
3
4
5
6

Fig 4. Mean vertical profiles of wind speed over the liquid surface for several airflow rates: ●, $0.07 \text{ m}^3 \text{ min}^{-1}$; ○, $0.28 \text{ m}^3 \text{ min}^{-1}$; ▼, $0.89 \text{ m}^3 \text{ min}^{-1}$; ▽, $1.41 \text{ m}^3 \text{ min}^{-1}$; ■, $1.69 \text{ m}^3 \text{ min}^{-1}$



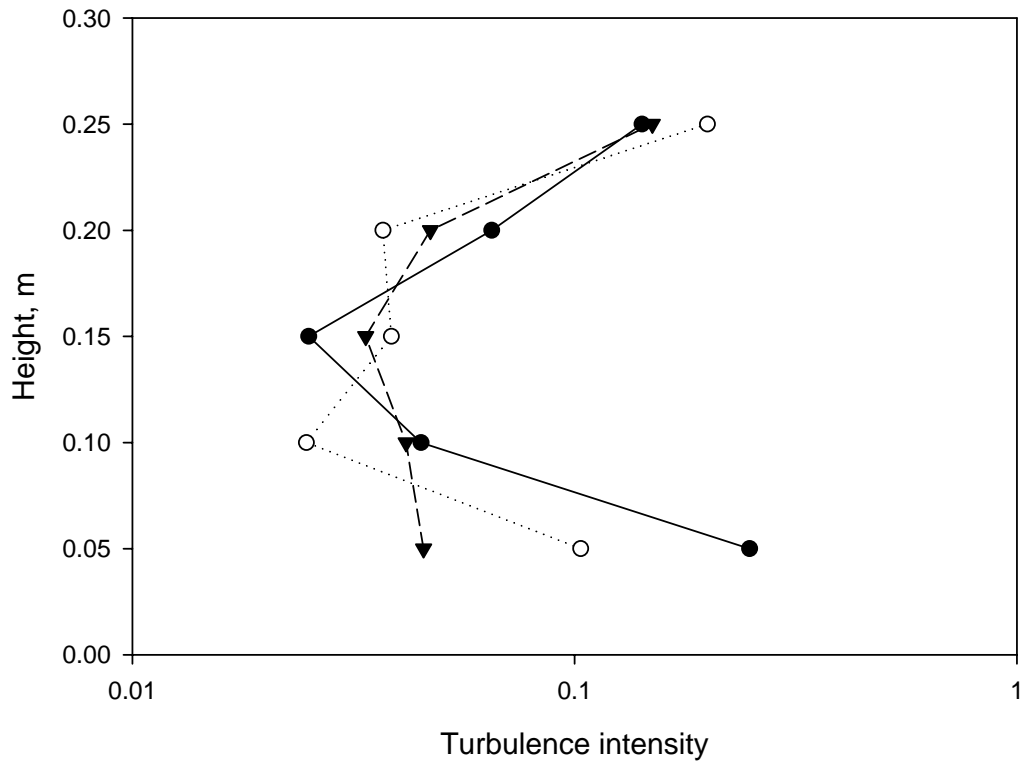
1
2
3
4

Fig 5. Contour map of cross-sectional wind speed over the solid surface at the airflow rate of $1.69 \text{ m}^3 \text{ min}^{-1}$. The unit of wind speed is m s^{-1}



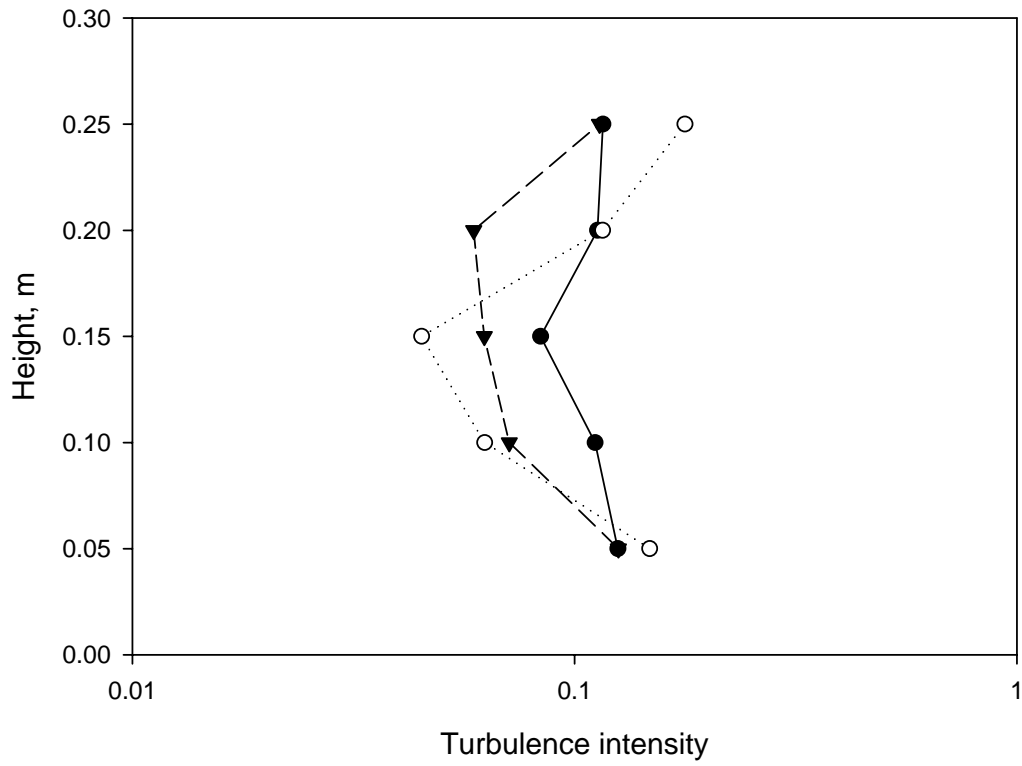
1
2
3
4

Fig 6. Contour map of cross-sectional wind speed profiles over the liquid surface at the airflow rate of $1.69 m^3 min^{-1}$. The unit of wind speed profiles is $m s^{-1}$



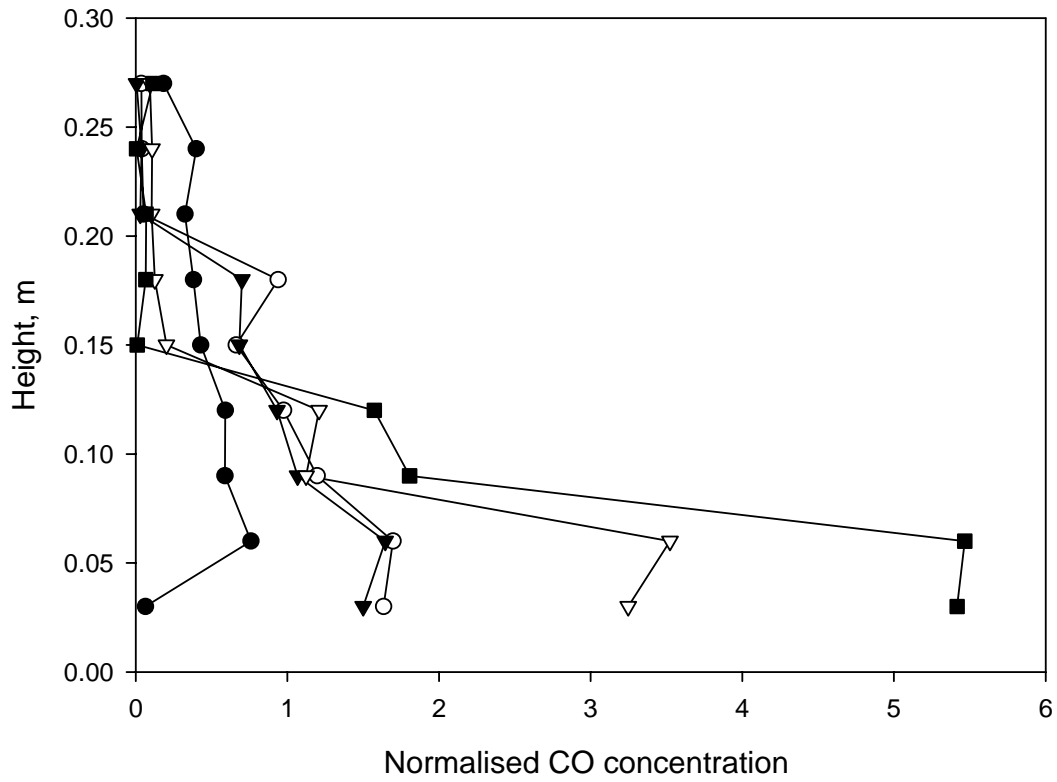
- 1
- 2
- 3
- 4
- 5

Fig 7. Turbulence intensity profiles over the solid surface: ●, $0.89 \text{ m}^3 \text{ min}^{-1}$; ○, $1.41 \text{ m}^3 \text{ min}^{-1}$; ▼, $1.69 \text{ m}^3 \text{ min}^{-1}$



1
2
3
4
5

Fig 8. Turbulence intensity profiles over the liquid surface: ●, $0.79 m^3 min^{-1}$; ○, $1.22 m^3 min^{-1}$; ▼, $1.69 m^3 min^{-1}$



1

2 *Fig 9. Normalised CO concentration profiles over the solid surface with a 5 litre min⁻¹*

3 *¹ CO supply rate: ●, 0.12 m³ min⁻¹; ○, 0.30 m³ min⁻¹; ▼, 0.78 m³ min⁻¹; ▽, 1.26 m³*

4 *min⁻¹; ■, 1.68 m³ min⁻¹*

1

2

Table 1.

3

Vertical and horizontal distances for wind speed sampling

<i>Cross sectional distances, m</i>	<i>Vertical distances, m</i>
0.08	0.05
0.17	0.10
0.25	0.15
0.33	0.20
0.42	0.25

4

1
2
3
4
5

Table 2.
Gas recovery efficiency of the tunnel for one point sampling port (port A) and 20
points four branched sampling port with quadratic distributed holes (port B)
with a CO supply rate of 5 litre min⁻¹

	<i>Port design</i>	<i>Airflow rate (m³ min⁻¹)</i>	<i>CO concentration (ppm)</i>		<i>Recovery efficiency (%)</i>
			<i>Theoretical</i>	<i>Measured</i>	
Test 1	A	0.07	14.24	2.85	20
	B			9.30	65
Test 2	A	0.28	4.02	0.68	17
	B			2.68	67
Test 3	A	0.89	1.27	0.79	62
	B			0.91	72
Test 4	A	1.41	0.78	0.51	65
	B			0.51	64
Test 5	A	1.69	0.67	0.54	81
	B			0.59	90

6